

Metal Complexes of *N*-Tosylamidoporphyrin: *cis*-Acetato-*N*-tosylimido-*meso*-tetraphenylporphyrinatothallium(III) and *trans*-Acetato-*N*-tosylimido-*meso*-tetraphenylporphyrinatogallium(III)

Jo-Yu Tung, Jyh-Iuan Jang, Chu-Chieh Lin, and Jyh-Horung Chen*

Department of Chemistry, National Chung-Hsing University, Taichung 40227, Taiwan, R.O.C

Lian-Pin Hwang

Department of Chemistry, National Taiwan University and Institute of Atomic and Molecular Sciences, Academia Sinica, Taipei 10764, Taiwan, R.O.C

Received September 22, 1999

The crystal structures of acetato-*N*-tosylimido-*meso*-tetraphenylporphyrinatothallium(III), $\text{Tl}(\text{N}-\text{NTs}-\text{tpp})(\text{OAc})$ (**1**), and acetato-*N*-tosylimido-*meso*-tetraphenylporphyrinatogallium(III), $\text{Ga}(\text{N}-\text{NTs}-\text{tpp})(\text{OAc})$ (**2**), were determined. The coordination sphere around the Tl^{3+} ion is a distorted square-based pyramid in which the apical site is occupied by a chelating bidentate OAc^- group, whereas for the Ga^{3+} ion, it is a distorted trigonal bipyramid with O(3), N(3), and N(5) lying in the equatorial plane. The porphyrin ring in the two complexes is distorted to a large extent. For the Tl^{3+} complex, the pyrrole ring bonded to the NTs ligand lies in a plane with a dihedral angle of 50.8° with respect to the 3N plane, which contains the three pyrrole nitrogens bonded to Tl^{3+} , but for the Ga^{3+} complex, this angle is found to be only 24.5° . In the former complex, Tl^{3+} and N(5) are located on the same side at 1.18 and 1.29 Å from its 3N plane, but in the latter one, Ga^{3+} and N(5) are located on different sides at -0.15 and 1.31 Å from its 3N plane. The free energy of activation at the coalescence temperature T_c for the intermolecular acetate exchange process in **1** in CD_2Cl_2 solvent is found to be $\Delta G_{171}^\ddagger = 36.0$ kJ/mol through ^1H NMR temperature-dependent measurements. In the slow-exchange region, the methyl and carbonyl (CO) carbons of the OAc^- group in **1** are separately located at δ 18.5 [$^3J(\text{Tl}-^{13}\text{C}) = 220$ Hz] and 176.3 [$^2J(\text{Tl}-^{13}\text{C}) = 205$ Hz] at -110 °C.

Introduction

Metalloporphyrins with a bridged structure between the central metal and one of the four pyrrole nitrogens have drawn much attention because it was proposed that the highly oxidized form of some hemoproteins may contain a ferric porphyrin with an oxygen atom inserted into an N–Fe bond.^{1,2} Only bridged metalloporphyrins with metal–N–N linkages (metal = Zn, Ni, Fe, Hg)^{3–8} have so far been reported. Callot³ and Mahy⁷ described the X-ray structure investigation of the metalation of *N*-tosylamido-*meso*-tetraphenylporphyrin [$\text{N}-\text{NHTs}-\text{Htp}$] (NHTs = tosylamido, tpp = dianion of *meso*-tetraphenylporphyrin, Ts = tosyl)⁹ leading to mononuclear complexes of

N-tosylimido-*meso*-tetraphenylporphyrinatonicel(II) [$\text{Ni}(\text{N}-\text{NTs}-\text{tpp})$] (NTs = tosylimido)³ and chloro-*N*-tosylimido-*meso*-tetraphenylporphyrinatoiron(III), $\text{Fe}(\text{N}-\text{NTs}-\text{tpp})\text{Cl}$ (or $\text{Fe}(\text{TPP})(\text{NTs})(\text{Cl})$, bridged).⁷ The nickel in $\text{Ni}(\text{N}-\text{NTs}-\text{tpp})$ is tetraordinated to three pyrrole nitrogens and one extra nitrogen atom from the nitrene fragment. The four pyrrole nitrogens are approximately coplanar. The nickel atom lies out of this four-nitrogen mean plane (4N) by 0.21 Å, and the extra nitrogen is also in the same direction with a distance of 0.94 Å. The porphyrin macrocyclic is distorted because of the nitrene insertion and because the perturbed pyrrole ring is oriented at a very large dihedral angle of 40.5° with respect to the 4N plane; the other three pyrroles are oriented at quite smaller angles of 1.8° , 4.4° , and 9.4° .³

The iron atom in $\text{Fe}(\text{N}-\text{NTs}-\text{tpp})\text{Cl}$ is pentacoordinated, and its coordination geometry is a distorted trigonal bipyramid with an equatorial plane containing three different atoms, Cl, N(Ts), and one pyrrole nitrogen. The porphyrin ring is also severely distorted as the pyrrole ring bonded to the NTs ligand orients in a dihedral angle of 29.9° with the 3N plane, which contains the three pyrrole nitrogens bonded to the iron.⁷

However, until now there are no X-ray structural data available for the diamagnetic metal ion (M(III)) complexes of $\text{N}-\text{NHTs}-\text{Htp}$ with coordination number (CN) above 4 (i.e., with $\text{CN} \geq 5$). In this paper, we present the results with the replacement of Ni(II) and Fe(III) with Ga(III) and Tl(III), respectively. This replacement causes the coordination

* To whom correspondence should be addressed.

- (1) Chevrier, B.; Lange, M.; Chottard, J. C.; Mansuy, D. *J. Am. Chem. Soc.* **1981**, *103*, 2899.
- (2) Setsune, J.; Ikeda, M.; Kishimoto, Y.; Ishimaru, Y.; Fukuhara, K.; Kitao, T. *Organometallics* **1991**, *10*, 1099.
- (3) Callot, H. J.; Chevrier, B.; Weiss, R. *J. Am. Chem. Soc.* **1978**, *100*, 4733.
- (4) Callot, H. J. *Tetrahedron* **1979**, *35*, 1455.
- (5) Ichimura, K. *Bull. Chem. Soc. Jpn.* **1978**, *51*, 1444.
- (6) Mahy, J. P.; Battioni, P.; Mansuy, D. *J. Am. Chem. Soc.* **1986**, *108*, 1079.
- (7) Mahy, J. P.; Battioni, P.; Bedi, G.; Mansuy, D.; Fishcher, J.; Weiss, R.; Morgenstern-Badarau, I. *Inorg. Chem.* **1988**, *27*, 353.
- (8) Callot, H. J.; Chevrier, B.; Weiss, R. *J. Am. Chem. Soc.* **1979**, *101*, 7729.
- (9) Au, S. M.; Fung, W. H.; Cheng, M. C.; Che, C. M.; Peng, S. M. *J. Chem. Soc., Chem. Commun.* **1997**, 1655.

number to increase from 4 for Ni^{II}(N–NTs–tpp)³ to 5 for *trans*-acetato-*N*-tosylimido-*meso*-tetraphenylporphyrinato-gallium(III) Ga(N–NTs–tpp)(OAc) (**2**) and from 5 for coordinated complex Fe(N–NTs–tpp)Cl⁷ to 6 for *cis*-acetato-*N*-tosylimido-*meso*-tetraphenylporphyrinatothallium(III) Tl(N–NTs–tpp)(OAc) (**1**). It is noted that the ionic radius increases from 0.69 Å for both Ni²⁺ and Ga³⁺ to 0.72 Å for Fe³⁺ and 1.025 Å for Tl³⁺.¹⁰ The relative positions of the OAc[−] and *N*-tosyl groups coordinated to the metal atom lead to a *cis* configuration in **1** and a *trans* configuration in **2** that might depend on the ionic radius of the Tl³⁺ and Ga³⁺. According to our previous report,¹¹ the ¹³C chemical shift of the carbonyl carbon of the acetato group in the diamagnetic complexes of M(por)(OAc)_{*n*} could indicate the axial binding mode. In addition, the ¹³C chemical shift of the β-pyrrole carbon (C_β) provides a complementary method for investigating the distortion of the *N*-pyrrole ring via the insertion of the nitrene moiety into the Tl⋯N bond in complex **1** and Ga⋯N bond in complex **2**. This paper reports (i) an X-ray structure determination that clearly establishes the Tl^{III}–NTs–N structure for the Tl(N–NTs–tpp)(OAc) complex and the Ga^{III}–NTs–N structure for the Ga(N–NTs–tpp)(OAc) complex and (ii) the ¹³C chemical shifts of the carbonyl carbon and the β-pyrrole carbon for further demonstration of the carboxylate coordination and the porphyrin macrocycle distortion, respectively. In addition, the ¹H and ¹³C NMR spectra of **1** in CD₂Cl₂ at low temperature are used to investigate the intermolecular apical ligand (OAc[−]) exchange process and in turn to determine the free energy of activation at the coalescence temperature, ΔG[‡]_{Tc}, for the exchange process.

Experimental Section

Preparation of Tl(N–NTs–tpp)(OAc) (1). Compound *N*-tosyl-amido-*meso*-tetraphenylporphyrin [N–NHTs–Htpp] was prepared as described in the literature.³ To a solution of Tl(OAc)₃ (45 mg, 0.118 mmol) and NaOAc (10 mg, 0.122 mmol) in CH₃OH (5 cm³) was added N–NHTs–Htpp (100 mg, 0.118 mmol) in CHCl₃ (20 cm³), and the resulting solution was refluxed for 30 min. After the solution was concentrated, it was dissolved in CHCl₃ and collected by filtration. Recrystallization from CHCl₃/MeOH afforded **1** as a purple solid (110 mg, 0.105 mmol, 87.5%). Compound **1** was dissolved in CHCl₃ and layered with MeOH. The purple and parallelepiped shape crystals of **1** were obtained for single-crystal X-ray analysis. Tables 1 and 2 summarize the ¹H and ¹³C NMR data. MS, *m/z* (assignment, rel intensity): 1045 ([Tl(N–NTs–tpp)(OAc)]⁺, 27.70), 986 ([Tl(N–NTs–tpp)]⁺, 31.23), 831 ([Tl(tpp) + N + H]⁺, 69.66), 817 ([Tl(tpp) + H]⁺, 72.23), 614 (Htpp⁺, 50.68), 205 (²⁰⁵Tl⁺, 100), 203 (²⁰³Tl⁺, 85.78). UV/visible spectrum, λ (nm) (ε × 10^{−3} (M^{−1} cm^{−1})) in CHCl₃: 446 (22.5), 558 (0.3), 602 (0.9).

Preparation of Ga(N–NTs–tpp)(OAc) (2). Free base N–NHTs–Htpp (150 mg) and Ga₂O₃ (200 mg) were refluxed for 1 h in 30 cm³ of acetic acid containing sodium acetate (150 mg). After removal of the solvent (HOAc) under reduced pressure, the residue was dissolved in CHCl₃ and then dried over Na₂SO₄. After filtration, the filtrate was rotavaped, and recrystallization from CHCl₃/*n*-hexane [1:6 (v/v)] afforded a purple solid of **2** (139.35 mg, 0.148 mmol, 86%). The crystals were grown by diffusion of ether vapor into a CHCl₃ solution. Tables 1 and 2 summarize the ¹H and ¹³C NMR data. MS, *m/z* (assignment, rel intensity): 850 ([Ga(N–NTs–tpp)–H]⁺, 21.90), 696 ([Ga(tpp) + N]⁺, 29.08), 681 ([Ga(tpp)]⁺, 100), 605 ([Ga(tpp) – C₆H₅ + H]⁺, 22.63). UV/visible spectrum, λ (nm) (ε × 10^{−3} (M^{−1} cm^{−1})) in CHCl₃: 436 (377), 544 (9.5), 587 (15.1), 635 (3.0).

Spectroscopy. Proton and ¹³C NMR spectra were recorded using CDCl₃ or CD₂Cl₂ at 300.00 (400.13 or 599.95) and 75.43 (100.61 or

150.87) MHz, respectively, on a Varian VXR-300 Bruker AM-400, or Varian Unity Inova-600 spectrometer. The temperature of the spectrometer probe was calibrated by the shift difference of methanol resonance in the ¹H NMR spectrum. ¹H–¹³C COSY was used to correlate protons and carbon through one-bond coupling and HMBC (heteronuclear multiple bond coherence) for two- and three-bond proton–carbon coupling.

The positive-ion fast atom bombardment mass spectrum (FAB MS) was obtained in a nitrobenzyl alcohol (NBA) matrix using a JEOL JMS-SX/SX 102A mass spectrometer.

Crystallography. Table 3 presents the crystal data as well as other information for Tl(N–NTs–tpp)(OAc) (**1**) and Ga(N–NTs–tpp)(OAc) (**2**). Measurements were taken on a Siemens R 3m/V diffractometer for **1** and on a Siemens SMART CCD diffractometer for **2** using monochromatized Mo Kα radiation (λ = 0.710 73 Å). Empirical absorption corrections were made for **1**. The structures were solved by direct methods (SHELXTL IRIS for **1** and SHELXTL PLUS for **2**) and refined by the full-matrix least-squares method. All non-hydrogen atoms were refined with anisotropic thermal parameters, whereas all hydrogen atom positions were calculated using a riding model and were included in the structure factor calculation. Table 4 lists selected bond distances and angles for both complexes.

Results and Discussion

Molecular Structures of 1 and 2. The skeletal frameworks are illustrated in Figure 1a for the complex Tl(N–NTs–tpp)(OAc)·0.75CHCl₃ with *P*₂/*c* symmetry and in Figure 1b for Ga(N–NTs–tpp)(OAc) (**2**) with *P*₁ symmetry. Their structures are a six-coordinate thallium and a five-coordinate gallium, having three nitrogen atoms of the porphyrins and one extra nitrogen atom of the nitrene fragment in common, but they are different with a chelating bidentate OAc[−] ligand for **1**·0.75CHCl₃ and a monodentate OAc[−] ligand for **2**. In compounds **1** and **2** it appears that the *N*-tosyl moiety is inserted into Tl–N and Ga–N bonds of acetato(*meso*-tetraphenylporphyrinato)thallium(III), Tl(tpp)(OAc),^{11–13} and acetato(*meso*-tetraphenylporphyrinato)gallium(III), Ga(tpp)(OAc).^{11,14} The unusual bond distances from Tl(III) and Ga(III) atoms to the ligand and the angles are summarized in Table 2. Bond distances (Å) are Tl–N(1) = 2.347(7), Tl–N(2) = 2.152(7), Tl–N(3) = 2.361(7), Tl–N(5) = 2.103(7), Tl–O(1) = 2.401(8), Tl–O(2) = 2.292(9), O(1)–C(21) = 1.22(2), O(2)–C(21) = 1.19(2), and C(21)–C(22) = 1.50(2) Å for **1**·0.75CHCl₃; they are Ga(1)–N(2) = 2.031(3), Ga(1)–N(3) = 1.911(3), Ga(1)–N(4) = 2.031(3), Ga(1)–N(5) = 1.946(3), Ga(1)–O(3) = 1.868(3), O(3)–C(52) = 1.260(5), O(4)–C(52) = 1.218(5), and C(52)–C(53) = 1.515(6) Å for **2**.

The geometry around Tl is a distorted square-based pyramid in which the apical site is occupied by a chelating bidentate OAc[−] group, whereas that around the Ga³⁺ is described as a distorted trigonal bipyramid with O(3), N(3), and N(5) lying in the equatorial plane. The distance between Ga(1) and O(4) is 2.865 Å. The pyrrole nitrogens N(4) and N(1) are no longer bonded to the thallium and gallium as indicated by their longer internuclear distances, 2.944 Å for Tl⋯N(4) and 2.641 Å for Ga(1)⋯N(1). The Tl–N(2) bond *trans* to the N(5) position in compound **1** is somewhat shorter than the other two Tl–N bond distances (i.e., 2.152(7) Å for Tl–N(2) compared to 2.347(7) Å for Tl–N(1) and 2.361(7) Å for Tl–N(3)). Likewise, the Ga(1)–N(3) bond in compound **2** is slightly shorter than the

(12) Chen, J. C.; Jang, H. S.; Chen, J. H.; Hwang, L. P. *Polyhedron* **1991**, *10*, 2069.

(13) Suen, S. C.; Lee, W. B.; Hong, F. E.; Jong, T. T.; Chen, J. H.; Hwang, L. P. *Polyhedron* **1992**, *11*, 3025.

(14) Hsieh, Y. Y.; Sheu, Y. H.; Liu, I. C.; Lin, C. C.; Chen, J. H.; Wang, S. S.; Lin, H. J. *J. Chem. Crystallogr.* **1996**, *26*, 203.

(10) Huheey, J. E.; Keiter, E. A.; Keiter, R. L. *Inorganic Chemistry*, 4th ed.; Harper Collins College: New York, 1993; p 114.

(11) Lin, S. J.; Hong, T. N.; Tung, J. Y.; Chen, J. H. *Inorg. Chem.* **1997**, *36*, 3886.

Table 1. ^1H NMR Data for Compounds **1**, **2**, N-NHTs-Htpp, and Ni(N-NTs-tpp)³ in CDCl_3 at 24 °C^a

compounds	H_β	H_β	H_β	$\phi\text{-H}$	H_β	tosyl- $\text{H}_{3,5}$	tosyl- $\text{H}_{2,6}$	tosyl- CH_3	OAc
N-NHTs-Htpp	9.01 (d, $^3J(\text{H-H}) = 5.2$ Hz)	8.93 (d, $^3J(\text{H-H}) = 4.4$ Hz)	8.79 s	8.42–7.75 m	7.90 s	6.43 (d, $^3J(\text{H-H}) = 8.0$ Hz)	4.90 (d, $^3J(\text{H-H}) = 8.0$ Hz)	2.12 s	
1	9.13 $\text{H}_{\beta(3,12)}^b$ (dd, $^4J(\text{TI-H}) = 18$ Hz $^3J(\text{H-H}) = 4.5$ Hz)	8.98 $\text{H}_{\beta(2,13)}$ (dd, $^4J(\text{TI-H}) = 10$ Hz $^3J(\text{H-H}) = 4.5$ Hz)	8.75 $\text{H}_{\beta(7,8)}$ (d, $^4J(\text{TI-H}) = 75.6$ Hz)	8.49–7.76 m	6.99 $\text{H}_{\beta(17,18)}$ s	6.96 (d, $^3J(\text{H-H}) = 7.5$ Hz)	6.26 (d, $^3J(\text{H-H}) = 7.5$ Hz)	2.31 s	0.67 s
2	9.29 $\text{H}_{\beta(9,10)}$ s	8.86 $\text{H}_{\beta(4,15)}$ (d, $^3J(\text{H-H}) = 4.8$ Hz)	8.81 $\text{H}_{\beta(5,14)}$ (d, $^3J(\text{H-H}) = 4.8$ Hz)	8.37–7.76 m	7.81 $\text{H}_{\beta(19,20)}$ s	6.47 (d, $^3J(\text{H-H}) = 7.8$ Hz)	4.80 (d, $^3J(\text{H-H}) = 7.8$ Hz)	2.11 s	–1.21 s
Ni(N-NTs-tpp)	8.74 s	8.72 (d, $^3J(\text{H-H}) = 4.5$ Hz)	8.65 (d, $^3J(\text{H-H}) = 4.5$ Hz)	8.35–7.65 m	7.31 s	6.55 (d, $^3J(\text{H-H}) = 8.0$ Hz)	5.38 (d, $^3J(\text{H-H}) = 8.0$ Hz)	2.14 s	

^a Chemical shifts in ppm relative to CDCl_3 at 7.24 ppm. s = singlet, d = doublet, m = multiplet, and dd = doublet of doublet. ^b $\text{H}_{\beta(a,b)}$ represents the two equivalent β -pyrrole protons attached to carbons a and b, respectively.

Table 2. ^{13}C NMR Data for Compounds **1** and **2** at 24 °C^a

compound	OAc CO	C_α	ϕ C_1	C_β	C_m	tosyl					ϕ $\text{C}_{2,6}, \text{C}_{3,5}, \text{C}_4$	OAc CH_3
						C_4	C_1	$\text{C}_{3,5}$	$\text{C}_{2,6}$	CH_3		
1 in CD_2Cl_2 (100.61 MHz)	176.6	157.5 [d, (C1,C14), 70] ^b	141.9 [d, 51] ^d	136.4 [d, (C3,C12), 38] ^c	128.0 [s, (C15,C20)]	143.2	137.5	129.4	127.3	21.3	137.7, 137.2, 135.7, 135.2,	19.8
		152.6 [d, (C16,C19), 72] ^c	141.6 [d, 48] ^d	133.8 [s, (C2,C13)]	124.4 [d, (C5,C10), 183] ^c		[d, 47] ^c				134.7, 134.3, 128.9,	
		150.5 [d, (C6,C9), 51] ^b	[C41,C31], [C51,C61]	132.3 [d, (C7,C8), 161] ^c							128.3, 127.2, 127.1	
		150.4 [d, (C4,C11), 102] ^b		115.6 [d, (C17,C18), 79] ^d								
2 in CDCl_3 (150.87 MHz)	168.7	149.3 (C3,C16)	142.3	135.0 (C5,C14)	123.5 (C2,C17)	141.2	135.3	128.0	124.9	21.1	137.3, 137.1, 135.7, 134.4,	19.2
		148.9 (C1,C18)	141.0,	133.2 (C9,C10)	122.4 (C7,C12)						128.4, 128.1, 128.0,	
		148.5 (C8,C11)	[C21,C39], [C27,C33]	129.8 (C4,C15)							127.1, 127.0, 126.9	
		147.1 (C6,C13)		119.7 (C19,C20)								

^a Chemical shifts in ppm relative to the center line of CDCl_3 at 77.0 and to CD_2Cl_2 at 53.6 ppm. ^b $^2J(\text{TI-C})$ in Hz. ^c $^3J(\text{TI-C})$ in Hz. ^d $^4J(\text{TI-C})$ in Hz.

Table 3. Crystal Data for $\text{Ti}(\text{N-NTs-tpp})(\text{OAc}) \cdot 0.75\text{CHCl}_3$ and $\text{Ga}(\text{N-NTs-tpp})(\text{OAc})$ (**2**)

empirical formula	$\text{C}_{53.75}\text{H}_{38.75}\text{Cl}_{2.25}\text{N}_5\text{O}_4\text{STi} \cdot 0.75\text{CHCl}_3$	$\text{C}_{53}\text{H}_{38}\text{GaN}_5\text{O}_4\text{S} \cdot 2$
fw	1134.8	1110.4
space group	$P2_1/c$	$P\bar{1}$
cryst syst	monoclinic	triclinic
<i>a</i> , Å	12.501(1)	11.5126(8)
<i>b</i> , Å	22.807(2)	12.9912(9)
<i>c</i> , Å	18.125(2)	16.786(1)
α , deg		82.661(1)
β , deg	90.94(2)	72.578(1)
γ , deg		73.461(1)
<i>V</i> , Å ³	5167(1)	2293.8(3)
<i>Z</i>	4	2
<i>F</i> ₀₀₀	2254	940
<i>D</i> _{calcd} , g cm ⁻³	1.459	1.319
$\mu(\text{Mo K}\alpha)$, cm ⁻¹	33.31	6.97
<i>S</i>	1.20	0.834
cryst size, mm ³	0.48 × 0.60 × 0.72	0.30 × 0.13 × 0.08
2 θ _{max} , deg	52.2	56.7
<i>T</i> , K	293	295(2)
no. reflns measd	10511	23483
no. reflns obsd	6093 (<i>F</i> > 4.0 σ (<i>F</i>))	10 396 (<i>I</i> > 2 σ (<i>I</i>))
<i>R</i> ^a %	4.87	5.43
<i>R</i> _w ^b %	5.85	9.15

^a $R = \sum ||F_o| - |F_c|| / \sum |F_o|$. ^b $R_w = [\sum w(|F_o| - |F_c|)^2 / \sum w(|F_o|)^2]^{1/2}$; $w = A / (\sigma^2 F_o + B F_o^2)$.

Table 4. Selected Bond Distances (Å) and Angles (deg) for Compounds $\text{Ti}(\text{N-NTs-tpp})(\text{OAc}) \cdot 0.75\text{CHCl}_3$ and $\text{Ga}(\text{N-NTs-tpp})(\text{OAc})$ (**2**)

$\text{Ti}(\text{N-NTs-tpp})(\text{OAc}) \cdot 0.75\text{CHCl}_3$			
Distances			
Ti–N(1)	2.347(7)	Ti–O(1)	2.410(8)
Ti–N(2)	2.152(7)	Ti–O(2)	2.292(9)
Ti–N(3)	2.361(7)	O(1)–C(21)	1.22(2)
Ti–N(5)	2.103(7)	O(2)–C(21)	1.19(2)
N(4)–N(5)	1.398(9)	C(21)–C(22)	1.50(2)
		N(5)–S	1.635(7)
Angles			
Ti–O(1)–C(21)	87.5(7)	O(2)–Ti–N(1)	138.5(3)
Ti–O(2)–C(21)	94.0(7)	O(2)–Ti–N(2)	92.1(3)
Ti–N(5)–N(4)	112.9(5)	O(2)–Ti–N(3)	100.9(3)
Ti–N(5)–S	129.1(4)	O(2)–Ti–N(5)	115.8(3)
O(1)–Ti–O(2)	53.8(3)	N(1)–Ti–N(2)	80.2(2)
O(1)–Ti–N(1)	88.2(3)	N(1)–Ti–N(3)	117.7(2)
O(1)–Ti–N(2)	103.3(3)	N(1)–Ti–N(5)	85.1(2)
O(1)–Ti–N(3)	154.1(3)	N(2)–Ti–N(3)	80.8(3)
O(1)–Ti–N(5)	102.3(3)	N(2)–Ti–N(5)	149.9(3)
		N(3)–Ti–N(5)	83.0(2)
$\text{Ga}(\text{N-NTs-tpp})(\text{OAc})$			
Distances			
Ga(1)–N(2)	2.031(3)	C(52)–O(3)	1.260(5)
Ga(1)–N(3)	1.911(3)	C(52)–O(4)	1.218(5)
Ga(1)–N(4)	2.031(3)	C(52)–C(53)	1.515(6)
Ga(1)–N(5)	1.946(3)	N(1)–N(5)	1.377(4)
Ga(1)–O(3)	1.868(3)	N(5)–S(1)	1.610(3)
Angles			
Ga(1)–O(3)–C(52)	117.3(3)	N(2)–Ga(1)–N(3)	92.9(1)
Ga(1)–N(5)–S(1)	137.9(2)	N(2)–Ga(1)–N(4)	168.7(1)
Ga(1)–N(5)–N(1)	103.9(2)	N(2)–Ga(1)–N(5)	83.2(1)
O(3)–Ga(1)–N(2)	89.5(1)	N(3)–Ga(1)–N(4)	93.9(1)
O(3)–Ga(1)–N(3)	128.2(1)	N(3)–Ga(1)–N(5)	126.9(1)
O(3)–Ga(1)–N(4)	93.4(1)	N(4)–Ga(1)–N(5)	85.5(1)
O(3)–Ga(1)–N(5)	104.8(1)		

other two Ga–N distances [1.911(3) Å for Ga(1)–N(3) vs 2.031(3) Å for the two equivalent Ga(1)–N(2) and Ga(1)–N(4) distances]. Figure 2 indicates the actual porphyrin skeleton for **1** and **2**; the four pyrrole nitrogens N(1)–N(4) are approximately coplanar (i.e., 4N plane) within ± 0.01 Å for **1** (Figure 2a) but

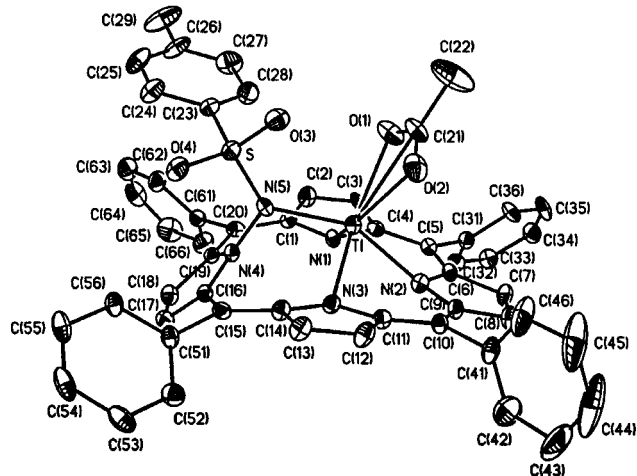
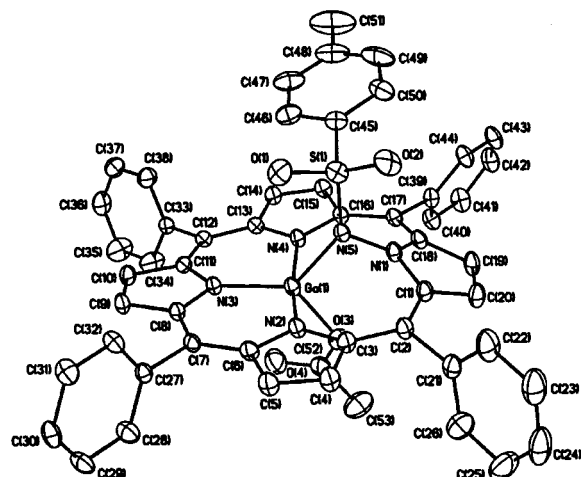
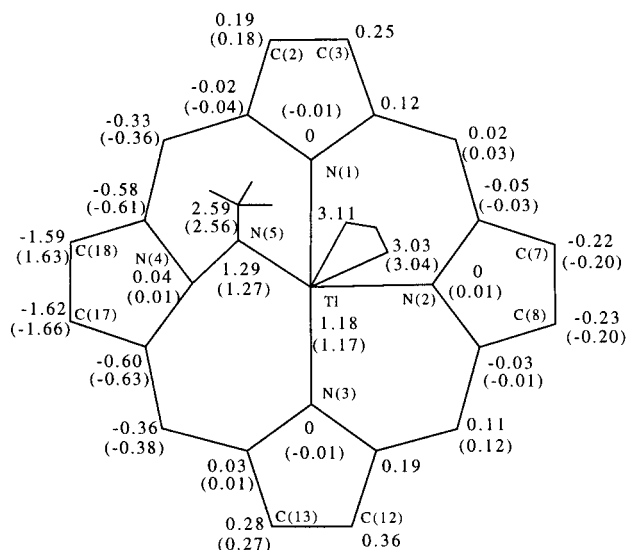
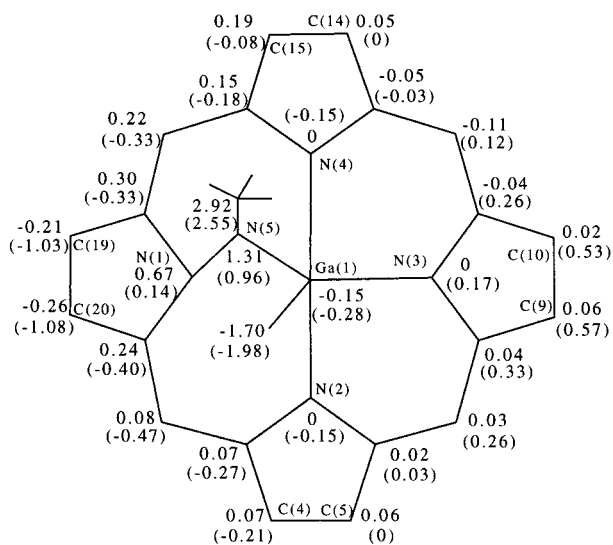
(a) $\text{Ti}(\text{N-NTs-tpp})(\text{OAc})$ (b) $\text{Ga}(\text{N-NTs-tpp})(\text{OAc})$

Figure 1. Molecular configuration and atom-labeling scheme for (a) $\text{Ti}(\text{N-NTs-tpp})(\text{OAc}) \cdot 0.75\text{CHCl}_3$ (or $1 \cdot 0.75 \text{CHCl}_3$) and (b) $\text{Ga}(\text{N-NTs-tpp})(\text{OAc})$ (**2**), with ellipsoids drawn at 30% probability. Hydrogen atoms for both compounds and solvents C(70)H(70a)Cl(1)–Cl(2)Cl(3) for $1 \cdot 0.75 \text{CHCl}_3$ are omitted for clarity.

± 0.15 Å for **2** (Figure 2b). The tosyl amide nitrogen N(5) in **1** and **2** are located considerably far from the (4N) plane. In complex **1**, Ti^{3+} and N(5) are located on the same side at 1.17 and 1.27 Å from its (4N) plane, but for complex **2**, Ga^{3+} and N(5) are located on different sides at -0.28 and 0.96 Å from its 4N plane (Figure 2). Apparently, chelating bidentate acetate in **1** is cis to the *N*-tosyl group with O(1) and O(2) being located separately at 3.11 and 3.04 Å out of the 4N plane, and monodentate acetate in **2** is trans to the *N*-tosyl group with O(3) located at -1.98 Å out of the 4N plane. The porphyrin macrocycle is indeed distorted because of the presence of the *N*-tosyl group. Thus, the N(4) and N(1) pyrrole rings bearing the *N*-tosyl group would deviate mostly from the (4N) plane and would be oriented separately in a dihedral angle of 51.3° and of 33.5° , whereas small angles of 6.0° , 7.4° , and 9.6° occur with N(2), N(1), and N(3) pyrroles for compound **1** and 4.8° , 8.1° , and 10.4° with N(4), N(2), and N(3) pyrroles for compound **2** (see also Table 5 in Supporting Information). In compound



(a) Tl(N-NTs-tpp)(OAc)



(b) Ga(N-NTs-tpp)(OAc)

Figure 2. Diagram of the porphyrinato core ($C_{20}N_4$, M, NTs, and OAc^-) of (a) compound **1** and (b) compound **2**. The values represent the displacements (in Å) of the atoms from the mean 3N plane (i.e., N(1)–N(3) for **1** and N(2)–N(4) for **2**) and the parenthesized values from the mean 4N plane (i.e., N(1)–N(4)).

1, such a large deviation from planarity for the N(4) pyrrole (Table 2) is also reflected by observing a 16–21 ppm upfield shift of the C_β (C17, C18) at 115.6 ppm compared to 136.4 ppm for C_β (C3, C12), 133.8 ppm for C_β (C2, C13), and 132.3 ppm for C_β (C7, C8). In compound **2**, a similar deviation is also found for the N(1) pyrrole (Table 2) by observing a 10–15 ppm upfield shift of the C_β (C19, C20) at 119.7 ppm compared to 135.0 ppm for C_β (C5, C14), 133.2 ppm for C_β (C9, C10), and 129.8 ppm for C_β (C4, C15). The distortion in **1** is larger than that present in the Ni(N-NTs-tpp) complex in which the dihedral angle between the mean plane of one pyrrole ring and the mean plane of the four pyrrole nitrogens (4N) is as large as 40.5°. Because of the larger size of the Tl^{3+} , the acetate ligand is bidentately chelated to the Tl atom, while it is unidentately coordinated to the Ga atom. Likewise, because of the same large size of the Tl^{3+} , Tl and N(5) lie 1.17 and 1.27 Å above the 4N

plane in **1** compared to 0.21 Å for Ni and 0.94 Å for the nitrogen atom of the nitrene fragment in Ni(N-NTs-tpp).³

The pyrrole ring nitrogens N(4) and N(1) are actually inclined toward the Tl and Ga atoms in **1** and **2**, respectively. These distortions re-form the distances between opposite pyrrole nitrogen atoms to be unusual. The normal diameter of the “hole” in an undistorted metalloporphyrin complex has been estimated to be 4.02 Å.¹⁵ In **1**, the N(2)···N(4) (or N(1)···N(3)) distance is 4.515 Å (or 4.029), and in **2** the N(1)···N(3) (or N(2)···N(4)) distance is 4.464 Å (or 4.042); it is caused by the large deviation of the N(4) pyrrole and N(1) pyrrole from the 4N plane for **1** and **2**, respectively. Hence, in **1** and **2**, the thallium(III) and gallium(III) atoms are all bound in an expanded porphyrinato (4N) core. The plane (*P*) defined by Tl, N(5), N(4), and the sulfur atom S, and the other plane by Ga(1), N(5), N(1), and S(1) are almost perpendicular to the (4N) plane, 84.4° for **1** and 90.3° for **2**. The tosyl group (T) (i.e., the plane *T*) is bonded to N(5) so that it lies above the macrocycle, orienting in a dihedral angle of 12.8° and 11.5° with the 4N plane in **1** and **2**, respectively (Table 5 in Supporting Information). The dihedral angles between the mean plane of the skeleton (4N) and the planes of the phenyl group are 55.7° (C(31)), 87.3° (C(41)), 34.7° (C(51)), and 50.1° (C(61)) for **1** and 73.0° (C(33)), 84.3° (C(27)), 75.4° (C(21)), and 57.4° (C(39)) for **2** (Table 5 in Supporting Information).

In comparison with a distorted trigonal bipyramidal structure of $Fe(N-NTs-tpp)Cl$,⁷ the individual planar pyrrole rings, bearing respectively the N(1), N(2), N(3), and N(4) nitrogen atoms in **2**, orient in dihedral angles of 24.5°, 1.7°, 2.2°, and 6.1° with respect to the 3N plane, which contains the three pyrrole nitrogens N(2), N(3), and N(4) bonded to the gallium (Table 5 in Supporting Information). This distortion is, however, smaller than that present in the $Fe(N-NTs-tpp)Cl$ complex in which the corresponding dihedral angles are 29.9°, 8.5°, 5.8°, and 9.8°, respectively.⁷ The pyrrole nitrogen N(1), not bonded to the gallium, lies 0.67 Å above the average plane of 3N (Figure 2b). Moreover, the gallium atom lies -0.15 Å below this plane toward the O(3) atom. In $Fe(N-NTs-tpp)Cl$,⁷ the corresponding pyrrole nitrogen N23 lies 0.44 Å above the 3N plane but the iron atom lies -0.21 Å below this plane toward the chlorine atom. Hence, the X-ray structure of compound **2** is quite similar to that of $Fe(N-NTs-tpp)Cl$ except that the latter is a paramagnetic complex.

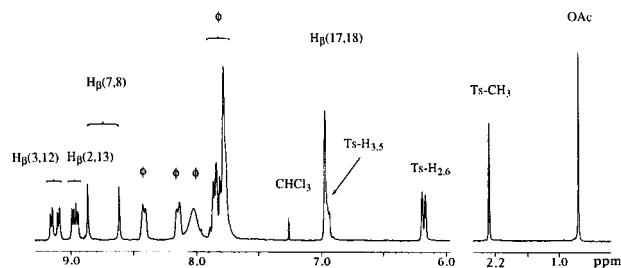
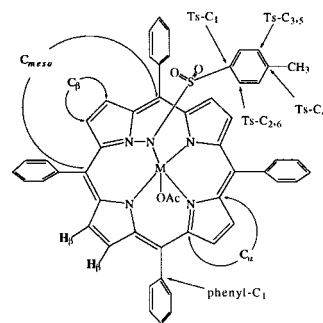
The distortion of the porphyrin skeleton seems to have very little or no effect at all on the π -electron delocalization in the porphyrinato core. By use of C_α and C_β to denote the respective α - and β -carbon atoms of a pyrrole ring, C_m for methine carbon, and C_p for a phenyl carbon atom that is bonded to the core, the averaged bond lengths in the porphine skeleton are N– C_α = 1.39(1) (or 1.376(4)), C_α – C_β = 1.43(1) (or 1.427(5)), C_β – C_β = 1.35(1) (or 1.347(5)), C_α – C_m = 1.41(1) (or 1.403(5)), and C_m – C_p = 1.50(1) Å (or 1.497(5)) for compound **1** (or **2**). These distances are almost identical with those found in nondistorted porphyrin complexes for $Tl(tpp)(OAc)$ ¹³ (or $Ga(tpp)(OAc)$).¹⁴ This has also been observed in the previously described porphyrin derivatives in which a nitrene moiety is inserted into a metal–pyrrole nitrogen bond.^{3,7,8}

The major difference between six-coordinate (**1**) and five-coordinate (**2**) complexes is the movement of the metal toward the 3N (or 4N) plane in the five-coordinate complex compared to the six-coordinate complex. In the binding to the OAc^- ligand in **2** with CN = 5, the smaller Ga(III) ion is forced to lie below

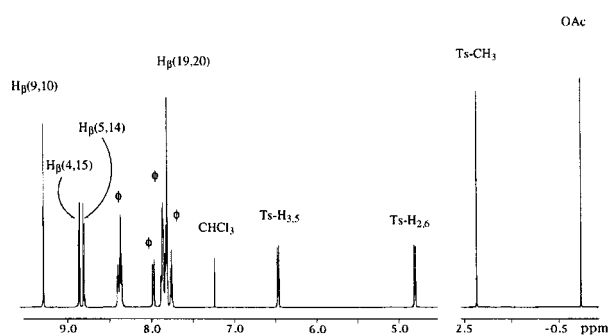
the 3N (or 4N) plane of the macrocycle. Hence, in **2** the distance between Ga and the 3N (or 4N) plane is only -0.15 (or -0.28) Å, while in **1** with CN = 6 this distance is much larger, ~ 1.18 (or ~ 1.17) Å for the larger Tl(III) ion.

¹H and ¹³C for Tl(N-NTs-tpp)(OAc) (1) and Ga(N-NTs-tpp)(OAc) (2) in CDCl₃ and CD₂Cl₂. Complexes **1** and **2** were characterized by ¹H and ¹³C NMR spectra. In solution, where the phenyl, *N*-tosyl, and acetate groups are free to rotate, the molecule has effective *C_s* symmetry with a mirror plane running through the N(2)–Tl–N(5)–N(4) unit for **1** or the N(3)–Ga(1)–N(5)–N(1) unit for **2**. There are four distinct β-pyrrole protons H_β, four β-pyrrole carbons C_β, four α-pyrrole carbons C_α, two different meso carbons C_{meso}, and two phenyl–C₁ carbons for both complexes (Tables 1 and 2). In compound **1**, the average distance between Tl···C(7) and Tl···C(8), Tl···C(3) and Tl···C(12), Tl···C(2) and Tl···C(13), and Tl···C(17) and Tl···C(18) increases from 4.258, 4.294, 4.415 to 4.712 Å. The NMR data of **1** showed four different types of Tl–H coupling constants for H_β (Figure 3 and Table 1). The doublet at 8.75 ppm is assigned as H_{β(7,8)} with ⁴J(Tl–H) = 75.6 Hz. The doublet of a doublet at 9.13 ppm is due to H_{β(3,12)} with ⁴J(Tl–H) = 18 Hz and ³J(H–H) = 4.5 Hz. The doublet of a doublet again at 8.98 ppm is due to H_{β(2,13)} with ⁴J(Tl–H) = 10 Hz and ³J(H–H) = 4.5 Hz, and the singlet at 6.99 ppm is due to H_{β(17,18)} with ⁵J(Tl–H) being unobserved. Likewise, there were also four different types of Tl–¹³C coupling constants for C_β (Table 2). The doublet at 132.3 ppm is due to C_β(C7, C8) with ³J(Tl–¹³C) = 161 Hz. The doublet at 136.4 ppm is due to C_β(C3, C12) with ³J(Tl–¹³C) = 38 Hz. The singlet at 133.8 ppm is due to C_β(C2, C13) with ³J(Tl–¹³C) being unobserved, and the doublet at 115.6 ppm is due to C_β(C17, C18) with ⁴J(Tl–¹³C) = 79 Hz. The ¹H NMR spectra (Figure 3) reveal that the aromatic protons of the tosyl groups appear as doublets at 6.96 (tosyl-H_{3,5}) and 6.26 ppm (tosyl-H_{2,6}) for **1** and at 6.47 and 4.80 ppm for **2**. All tosylimido and acetate protons are shifted upfield compared to their counterparts on free NHTs and OAc[−]. Such a shift is presumably attributed to the porphyrin ring current effect. On the basis of the ring model,¹⁶ as the distance between the geometrical center (C_t) of the 4N plane and axial protons gets smaller, the shielding effect becomes larger. The (C_t···axial proton) distance can be estimated from C_t to the carbons bearing the axial protons. The average distances (in Å) for C_t···tosyl-C_{2,6}, C_t···tosyl-C_{3,5}, C_t···tosyl-CH₃, and C_t···CH₃ (OAc) are 5.282, 6.364, 8.159, and 5.374 in **1**, and 4.397, 5.424, 7.190, and 4.339 in **2**. The fact that all four bond distances in **2** are shorter than those in **1** indicates that the ring current effect in **2** would be larger and in turn the ¹H upfield shifts for the axial protons in **2** would be still higher. This is what exactly observed: -1.21 ppm in **1** and 0.78 ppm in **2** for OAc, 2.11 and 2.31 for tosyl-CH₃, 4.80 and 6.26 for tosyl-H_{2,6}, and 6.47 and 6.96 for tosyl-H_{3,5}. The above ring current effect indicates that both the tosyl and acetate ligands are bonded to Tl in **1** and to Ga in **2**. This bonding argument is further confirmed by the result that the tosyl-C₁ (i.e., C(23)) in **1** was observed at 137.5 ppm with ³J(Tl–C) = 47 Hz.

Dynamical NMR of 1 in CD₂Cl₂. When a 0.02 M solution of Tl(N-NTs-tpp)(OAc) (**1**) in CD₂Cl₂ (Figure 4) was recorded at low temperature, the methyl protons of OAc[−] appeared as a single peak at 24 °C ($\delta = 0.67$ ppm). At -110 °C the singlet first broadened (coalescence temperature $T_c = -102$ °C) and then split into two peaks with a separation of 16.2 Hz. Since the exchange of OAc[−] within **1** is reversible, the results observed at 599.95 MHz confirm that the separation results from a



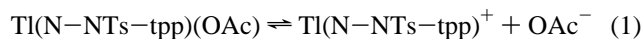
(a)



(b)

Figure 3. ¹H NMR spectra for (a) Tl(N-NTs-tpp)(OAc) (**1**) at 299.94 MHz and (b) Ga(N-NTs-tpp)(OAc) (**2**) at 599.95 MHz in CDCl₃ at 24 °C. ϕ represents the phenyl protons.

coupling of ⁴J(Tl–H) rather than a chemical shift difference. The most likely cause of loss of coupling is reversible dissociation of acetate



with a small dissociation constant but reasonable rate at room temperature.¹⁷ Such a scenario would lead to little change in the chemical shift with temperature and no detectable free OAc[−] and Tl(N-NTs-tpp)⁺ at low temperature but would result in the loss of coupling between acetate and thallium at higher temperatures. The chemical shift observed at high temperature

(17) Jenson, J. P.; Muetterties, E. L. In *Dynamic Nuclear Magnetic Resonance Spectroscopy*; Jackman, L. M., Cotton, F. A., Eds.; Academic Press: New York, 1975; pp 299–304.

(16) Johnson, C. E.; Bovey, F. A. *J. Chem. Phys.* **1958**, *29*, 1012.

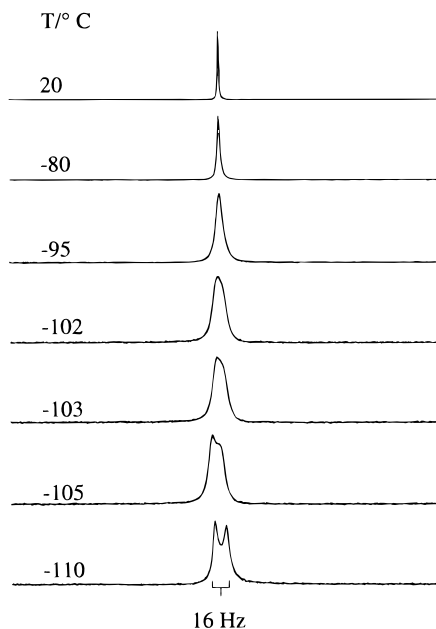


Figure 4. The 599.95 MHz ^1H NMR spectra for the axial acetato protons of $\text{Tl}(\text{N-NTs-tpp})(\text{OAc})$ (**1**) in CD_2Cl_2 at various temperatures.

is the average of two species (i.e., $\text{Tl}(\text{N-NTs-tpp})(\text{OAc})$ and OAc^-) in eq 1 weighted by their concentration. A comparison of observed and computed spectra yields $\Delta G^\ddagger_{171} = 36.0$ kJ/mol. At 24 °C, intermolecular exchange of the OAc^- group is rapid, indicated by singlet signals due to carbonyl carbons at 176.4 ppm and methyl carbons at 19.1 ppm. At -110 °C, the rate of intermolecular exchange of OAc^- for **1** in CD_2Cl_2 is slow. Hence, at this temperature, the methyl and carbonyl carbons of OAc^- are observed at 18.5 ppm [with $^3J(\text{Tl}-\text{C}) = 220$ Hz] and 176.3 ppm [with $^2J(\text{Tl}-\text{C}) = 205$ Hz], respectively. These ^{13}C resonances are quite close to the $\text{Tl}(\text{tpp})(\text{OAc})$ case in which the two corresponding carbons were observed, in CD_2Cl_2 at -90 °C, at 18.8 ppm [with $^3J(\text{Tl}-\text{C}) = 280$ Hz], and 174.9 ppm [with $^2J(\text{Tl}-\text{C}) = 235$ Hz].^{12,13} For **2** in CDCl_3 at 24 and -50 °C, the corresponding carbons were observed at 19.2 and 168.7, close to those of 20.4 ppm (CH_3) and 168.8 ppm (CO) in $\text{Ga}(\text{tpp})(\text{OAc})$.¹⁴ On the basis of our previous report,¹¹ the carbonyl chemical shifts at 176.4 ppm (within the

value of 175.2 ± 1.6 ppm) for **1** and at 168.7 (within the range of 168.2 ± 1.7 ppm) for **2** at 24 °C also confirm that the OAc^- group is bidentately chelated to the Tl atom but unidentately coordinated to the Ga atom.

UV/Visible Absorption Spectra of 1 and 2. The electronic spectrum of **1** in CHCl_3 has three λ_{max} at 446 (B(0,0)), 558 (Q(1,0)), and 602 (Q(0,0)) that are comparable to those of 433, 567, and 607 nm found for $\text{Tl}(\text{tpp})(\text{OAc})$,^{18,19} a cisoid six-coordinate thallium(III) porphyrin complex. On the other hand, the electronic spectrum of **2** has three λ_{max} at 436 (B(0,0)), 544 (Q(1,0)), and 587 (B(0,0)), which are also quite closer to those of 420, 552, and 586 for $\text{Ga}(\text{tpp})(\text{OAc})$,²⁰ a typical five-coordinate gallium(III) porphyrin complex.

Conclusions

We have investigated two novel diamagnetic, mononuclear, and bridged metal complexes of *N*-tosylamidoporphyrin having an $\text{M}^{\text{III}}-\text{NTs}-\text{N}$ linkage, and their X-ray structures are studied. The ^{13}C chemical shifts of the carbonyl carbon are used to identify the coordinate mode of the acetato group. Dynamical ^1H and ^{13}C NMR spectra of the acetato group in **1** reveal that this group undergoes an intermolecular exchange with a free energy of activation, $\Delta G^\ddagger_{171} = 36.0$ kJ/mol.

Acknowledgment. The financial support from the National Research Council of the R.O.C. under Grant NSC 89-2113-M-005-014 is gratefully acknowledged. The NMR instrument (Varian Unity Inova-600) is funded in part by the National Science Council and by the Chung-Cheng Agriculture Science & Social Welfare Foundation.

Supporting Information Available: Table 5 giving least-squares mean planes and the dihedral angles between planes for compounds **1** and **2**. X-ray crystallographic files for compounds **1** and **2** are available in CIF format. This material is available free of charge via the Internet at <http://pubs.acs.org>.

IC9911318

- (18) Abraham, R. J.; Barnett, G. H.; Smith, K. M. *J. Chem. Soc., Perkin Trans. 1* **1973**, 2142.
- (19) Tung, J. Y.; Chen, J. H.; Liao, F. L.; Wang, S. L.; Hwang, L. P. *Inorg. Chem.* **1998**, *37*, 6104.
- (20) Yang, F. L.; Li, P.; Lin, X. Q.; Wang, E. K. *Chin. Chem. Lett.* **1993**, *4*, 119.